

Clustering Properties in Turbulent Signals

K. R. Sreenivasan¹ and A. Bershadskii^{1,2}

Received August 29, 2005; accepted April 5, 2006

Published Online: July 12, 2006

We consider the telegraph approximation (TA) of turbulent signals by ignoring their amplitude variability and retaining only their ‘zero’-crossing information. We establish a unique relationship between the spectral exponent of a signal and that of its TA, whenever the signal possesses a Gaussian PDF and a spectral shape in which the high-frequency cut-off is sufficiently sharp. The velocity signals in most turbulent flows away from the wall satisfy these conditions approximately, so that the Kolmogorov spectral exponent of $-5/3$ for the turbulent velocity spectrum corresponds to a $-4/3$ spectral exponent for its TA. By introducing a new scaling exponent to characterize the tendency of small-scale fluctuations to cluster, we show that the velocity and passive scalar signals display a finite tendency to cluster even in the limit of $Re \rightarrow \infty$. We advance the notion, on the basis of the properties of the TA, that turbulent processes belong to one of two classes—either the ‘white noise’ type or the ‘Markov-Lorentzian’ type.

KEY WORDS: clustering, intermittency, zero-crossings, turbulence

PACS: 47.27.-i, 47.27.Gs, 47.27.Nz

1. INTRODUCTION

Understanding scaling laws of turbulence is still a challenging problem. Basic properties such as spectral distribution in the scaling region of the turbulent energy have not yet been obtained from the Navier-Stokes equations analytically. For instance, one does not yet know, analytically, if the cornerstone of turbulence theory, namely Kolmogorov’s $-5/3$ spectral law in the inertial range of scales,⁽¹³⁾ is correct or needs profound modifications. Inertial range is the range of scales that are not affected directly either by the injection of energy by forcing or its removal by dissipation. The invariant in that range of scales is the average flux of energy across scales, which, in the steady state, equals the injection rate as well as the dissipation rate.

¹ International Center for Theoretical Physics, Strada Costiera 11, I-34100 Trieste, Italy

² ICAR, P.O. Box 31155, Jerusalem 91000, Israel

The situation with respect to intermittency is arguably even more acute. Intermittency means that small-scale quantities, such as the energy dissipation, are distributed unevenly in space—perhaps also in time. It is thought that this property of turbulence (also surmised to be true for other nonlinear dynamical systems) introduces a powerful shift from critical phenomena. The empirical observation of multiscaling, thought to be the manifest property of intermittency, begs one to discover, potentially, a multiplicity of broken symmetries of the governing equations.⁽⁸⁾

These broad issues are beyond the scope of the present paper, which is meant as a contribution to a specific aspect of intermittency. The original aspect of the contribution is the proposed simplification of the problem using the so-called telegraph approximation to the measured velocity signals, as described below. As we shall show using data from experiments and numerical simulations, the telegraph approximation can effectively separate two main components of intermittency—one related to the amplitude of small-scale fluctuations, and another to the local frequency of oscillations. Usually, an underlying multifractal distribution exists for the former while the latter is associated with a monofractal tendency of events to cluster together.

In this paper, we regard time traces of turbulent quantities such as velocity and temperature as equivalent to one-dimensional spatial cuts. This so-called Taylor's hypothesis has a long and venerable history in the turbulence literature.⁽¹⁷⁾ This hypothesis states that the intrinsic time dependence of the velocity or temperature field can be ignored when the turbulence is convected past the probes at nearly constant speed. With this hypothesis, the temporal dynamics should reflect the spatial one. Small-scale and high-frequency fluctuations are then regarded interchangeably.

We first generate the telegraph approximation (TA) of turbulent signals, which, as mentioned above, assists us in separating the clustering tendency from amplitude effects. TA ignores the variation of amplitude from one excursion of the signal to another and replaces the experimental signal of the type shown in the upper part of Fig. 1 by that shown in its lower part. This approximation is generated from the measured signal by setting the magnitudes to 1 or 0 depending on whether the actual magnitude exceeds the mean value (marked as zero without any loss of generality and shown by the dashed line in the top part of Fig. 1). Formally, for a measured quantity $v(t)$ (with zero mean), the telegraph approximation $u(t)$ is constructed as

$$u(t) = \frac{1}{2} \left(\frac{v(t)}{|v(t)|} + 1 \right).$$

By definition, TA can only assume either 1 or 0.

We shall show that the spectral scaling of TA can give significant information about the spectral scaling of the full signal in the inertial range (Sec. 2). We

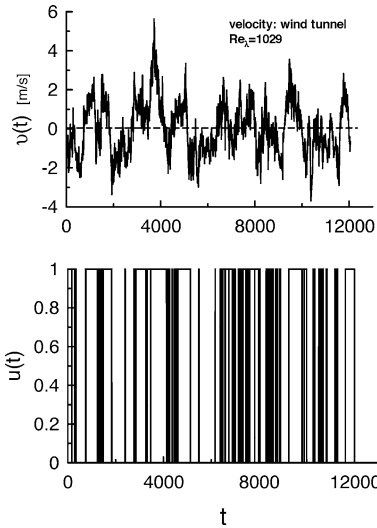


Fig. 1. Example of the velocity fluctuations signal (*upper part*) and its telegraph approximation.

characterize the clustering properties of TA in Sec. 3 and discuss their applications in Sec. 4. Section 5 examines the probability density function for time intervals between pulses. Concluding remarks are presented in Sec. 6.

2. SPECTRA

We show in Fig. 2a the power spectral density for the velocity measured in the atmospheric surface layer at a Taylor microscale Reynolds number $Re_\lambda = 19,000$.⁽²⁴⁾ The microscale Reynolds number is proportional to the square-root of the large-scale Reynolds number. The straight line is the “ $-5/3$ ” Kolmogorov spectral form in the inertial range.⁽¹⁷⁾ Figure 2b shows the spectrum of the TA of the signal, and the straight line there shows the “ $-4/3$ ” scaling. We verified from turbulent velocity signals measured at different Reynolds numbers that all their TAs show the “ $-4/3$ ” slope (though, of course, the range of applicable scales increases with the Reynolds number). In all the cases examined, we observed a more extensive scaling in the TA than in the full signal itself.

To examine the correspondence between the spectral slope of the full signal and that of its TA, we numerically generated several stochastic signals with various spectral roll-off rates and obtained the spectral scaling of their TAs. Because turbulent velocity fluctuations measured away from a solid wall possess roughly Gaussian probability density function (PDF), and the numerical signals possessed a Gaussian distribution of amplitudes and their high-frequency part decayed rapidly

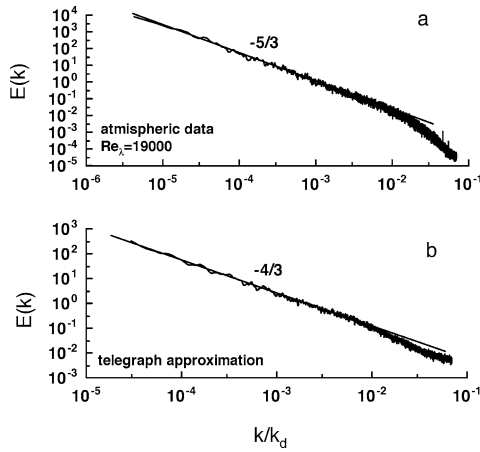


Fig. 2. Spectrum of (a) the velocity fluctuations and (b) of its telegraph approximation. The velocity data are obtained in slightly unstable atmospheric surface layer; the microscale Reynolds number $R_\lambda = 19,000$. The non-scaling low frequency part of the spectrum is not shown (simply because the finite FFT length used for these calculations did not contain enough large scales). It has been shown in⁽²⁴⁾ that the low-frequency part flattens out which, in this loose sense, is similar to white noise. k_d is the Kolmogorov wavenumber.

(as it does for turbulence, see Fig. 2a), we observed a unique relationship between the spectral exponent, n , of the full signal and that of its TA, m (say). The relation is

$$m = \frac{n + 1}{2}. \quad (1)$$

This relation is based on numerical results but should be provable analytically for certain classes of stochastic processes. In the Appendix, we present a heuristic proof.⁽⁶⁾ It should, however, be noted that the class of stochastic processes for which this relation is valid is still undefined and rigorous definition of this class can be a difficult problem.^(3,9,16) Incidentally, the result holds numerically for passive scalars as well.

We may speculate about one possible usefulness of this result. We suppose that it is easier to obtain (perhaps using symbolic dynamics or similar methods) certain types of analytical results for TA for the Navier-Stokes velocity, rather than for the velocity itself. From such exercises, if the inertial-range scaling exponent for TA of the velocity can be shown to be $-4/3$ (or a close approximation to it), it would mean that the Kolmogorov spectral exponent of $-5/3$ (or a close approximation to it) for the Navier-Stokes velocity would be one step closer to being an analytical result.

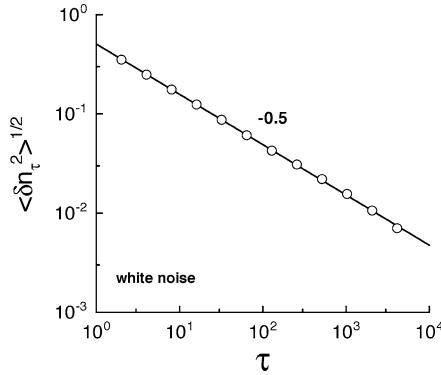


Fig. 3. Standard deviation of the running density fluctuations against τ for white noise.

3. THE CLUSTER EXPONENT

We now turn to the clustering information that can be extracted from TA. Let us count the number of ‘zero’-crossing points of TA (the same as the ‘zero’-crossing points of the full signal) in a time interval τ and consider their average density n_τ . Let us denote fluctuations of the running density as $\delta n_\tau = n_\tau - \langle n_\tau \rangle$, where the brackets mean the average over long times. We are interested in the variation of the standard deviation of the running density fluctuations $\langle \delta n_\tau^2 \rangle^{1/2}$ with τ .

For reference, Fig. 3 shows the result for the white noise signal, which, presumably, has no clustering. The straight line is the scaling relation

$$\langle \delta n_\tau^2 \rangle^{1/2} \sim \tau^\alpha, \tag{2}$$

with $\alpha = 1/2$. This result for white noise can be derived analytically.^(2,14,16)

In Fig. 4 we show results from analogous calculations for the turbulent velocity signals obtained in a wind-tunnel experiment⁽¹⁹⁾ for different Reynolds numbers. Two scaling intervals of the type (2) appear, and the straight lines show the two values of the exponent α . The scaling interval to the left covers dissipative and inertial ranges, and that to the right covers scales larger than the integral scale of the flow. The latter has an exponent of 1/2. This is not surprising because the large scales behave like white noise. We can therefore regard the large scales as having no clustering properties, and shall ignore them further. On the other hand, the scaling on the left (with $\alpha < 1/2$) indicates the tendency of small scales to cluster. The cluster exponent α for small scales decreases with increasing Re_λ , which means an increasing tendency to cluster (as was expected from visual inspection). There is no analytical proof for this result for turbulence.

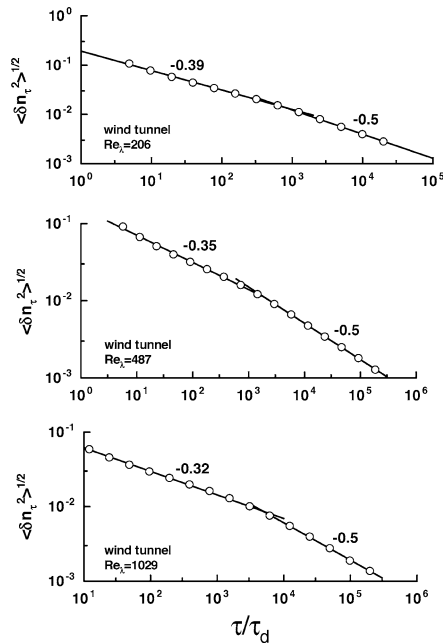


Fig. 4. As in Fig. 3 but for velocity signals obtained in a wind tunnel experiment⁽¹⁹⁾ at different values of Reynolds numbers. τ_d is the timescale equivalent to the Kolmogorov length scale.

4. APPLICATIONS OF THE CLUSTER EXPONENT

An intriguing question concerns the limiting value of α as $Re_\lambda \rightarrow \infty$. It is natural to consider the functional relation $\alpha = \alpha(\ln Re_\lambda)$. We have explored in some detail elsewhere⁽²³⁾ the question of why logarithmic expansions such as this are relevant to turbulence; we have also shown that in circumstances governed by vortex instabilities, the use of $\ln Re_\lambda$ is the appropriate expansion parameter instead of Re_λ itself. The idea was earlier explored in wall flows in Ref. 1. Expanding α for large Re_λ in power series as

$$\alpha(\ln Re_\lambda) = \alpha_\infty + \frac{a_1}{\ln Re_\lambda} + \frac{a_2}{(\ln Re_\lambda)^2} + \dots, \tag{3}$$

and, keeping only the first two terms, we show in Fig. 5 the calculated values of α against $1/\ln Re_\lambda$ for velocity signals in the range $200 < Re_\lambda < 20000$. The straight line given by

$$\alpha(\ln Re_\lambda) \simeq 0.1 + \frac{3/2}{\ln Re_\lambda} \tag{4}$$

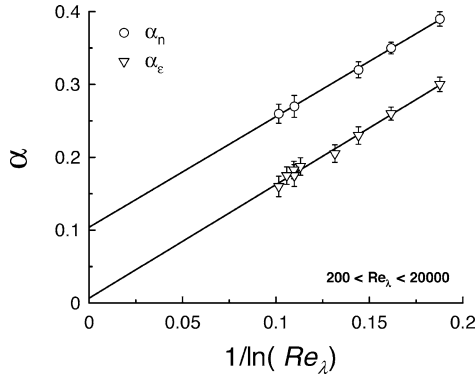


Fig. 5. The cluster exponent α (circles) against $1/\ln Re_\lambda$ for velocity signal in the Reynolds number range $200 < Re_\lambda < 20,000$; $\alpha_\infty \approx 0.1$; $\alpha_1 \approx \frac{3}{2}$. The scaling exponents α_ε (triangles) are for the dissipation fluctuations computed from the *full* signals; $\alpha_{\varepsilon\infty} \approx 0$; $\alpha_{\varepsilon 1} \approx \frac{3}{2}$.

fits the data very well. In particular, we have

$$\lim_{Re_\lambda \rightarrow \infty} \alpha \equiv \alpha_\infty \simeq 0.1. \tag{5}$$

The finiteness of α_∞ supports the notion that the limiting case of $Re_\lambda \rightarrow \infty$ is qualitatively no different from the case of finite Reynolds numbers with respect to its clustering properties.

For comparison we also show in Fig. 5 the scaling exponents calculated for the dissipation rate computed from the *full* velocity signals

$$\langle \delta \varepsilon_\tau^2 \rangle^{1/2} \sim \tau^{\alpha_\varepsilon}, \tag{6}$$

where we have used

$$\varepsilon_\tau = \frac{\int_0^\tau \varepsilon(t) dt}{\tau}. \tag{7}$$

This local average was introduced by Obukhov⁽¹⁸⁾ to describe intermittency. We have also added four data points for α_ε for a mixing layer⁽²⁰⁾ and the atmospheric surface layer.⁽²⁴⁾ One can see that for the dissipation, the limit is close to trivial: $\lim_{Re \rightarrow \infty} \alpha_\varepsilon \approx 0$ (cf. Refs. 1, 4, 15).

It is worth emphasizing that the scaling exponent α_ε of Fig. 5 corresponds to the dissipation rate computed from the *full* velocity signals. Therefore, the similarity of cluster exponent α and α_ε is remarkable. This means, in particular, that, at least for $Re_\lambda > 200$, we have the simple relationship

$$\alpha_\varepsilon(Re_\lambda) = \alpha(Re_\lambda) + c, \tag{8}$$

where $c \simeq -0.1$ is independent of Re_λ . The implication is that there is simple splitting of the intermittency exponent α_ε between $\alpha_n(Re_\lambda)$, which is connected with clustering properties, and the component c which is independent of Re_λ and the flow, hence perhaps deserves the designation of being ‘universal.’ Therefore, to within this universal constant, the clustering of small-scale velocity fluctuations alone determines the Reynolds number dependence of intermittency.

One can also use Eq. (4) to obtain a bound $Re_\lambda^{(c)}$ on the Reynolds number at which a non-trivial exponent would begin to appear. The bound can be obtained from the equation

$$\alpha(\ln Re_\lambda^{(c)}) \simeq 0.1 + \frac{3/2}{\ln Re_\lambda^{(c)}} = 1/2, \tag{9}$$

which gives us

$$Re_\lambda^{(c)} \simeq 42. \tag{10}$$

The value seems reasonable because it is roughly equal to the minimum Reynolds number at which a flow begins to attain other characteristics of fully developed turbulence.⁽²¹⁾

The clustering tendency of small scales of the passive scalar in turbulent flows can also be characterized by the cluster-exponent, as can be seen in Fig. 6. Data shown in Fig. 6a were calculated from a signal acquired with a cold-wire probe in the wake of a heated cylinder in a wind tunnel at $Re_\lambda \simeq 130$ (see Ref. 11 for details of the experiment). Temperature can be considered as a passive scalar

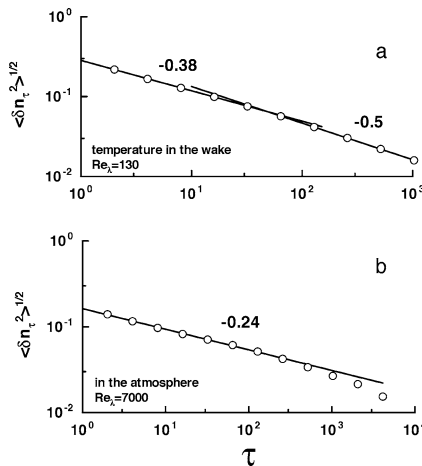


Fig. 6. As in Fig. 3 but for temperature (passive scalar) fluctuations measured in the turbulent wake at $Re_\lambda = 130$ (Fig. 6a), and in unstable atmospheric surface layer at $Re_\lambda = 7000$ (Fig. 6b).

for the conditions of this experiment. Data shown in the Fig. 6b were obtained from a temperature signal measured in the unstable atmospheric surface layer at $Re_\lambda \simeq 7000$.⁽¹²⁾ The straight lines are drawn in order to compare the data with Eq. (2).

The Reynolds number variation of the cluster exponent for the passive scalar can be discussed using Eq. (3). Data not presented here show that the first two terms of Eq. (3) give the same slope ($\approx \frac{3}{2}$) as for velocity but $\alpha_{\varepsilon_\infty} \simeq 0.07$. This means, in particular, that the small-scale fluctuations of passive scalar are more strongly clustered than the velocity fluctuations at the same Reynolds number. This is consistent with the tendency of the scalars to form ramp-cliff structures.⁽²²⁾

5. PROBABILITY DENSITY FUNCTIONS OF THE INTERPULSE PERIOD

Recall that the scaling exponent of the spectrum of the TA is determined completely by that of the spectrum of the full signal (Sec. 2). In contrast, the cluster exponents of the TA signals depend on the interplay between the scaling part of the full spectrum and its dissipative part. Moreover, the cluster exponent can exist for TA even when the original spectrum does not exhibit any scaling, and may indeed contain substantial qualitative information about the full signal. This requires that we consider the distribution of the crossing intervals of TA (same as the crossing intervals of the original signal). This distribution does not have any information about the ordering of events in space (or time)—unlike the cluster exponent.

We consider the probability density function (PDF) of the crossing intervals between pulses τ (i.e. interval of time between two successive zero-crossing points). The pulses can also be characterized by the return time T ($T = \tau_i + \tau_{i+1}$, where i is index of the zero-crossing point in the time series).

In Sec. 3 we compared the tendency of turbulent signals to cluster with white noise as a model of disorder. It is interesting to continue this comparison with respect to the PDF of T . If the white noise is a model signal for the turbulence *in this respect*, the PDFs should be similar. Figure 7 shows, as an example, $p(T)$ for a white noise signal (Fig. 7a), for the passive scalar signal (Fig. 7b), and for the velocity signal (Fig. 7c). The solid lines are the best fit to a lognormal distribution. One can see that the central parts of the PDFs are indeed similar for all three signals. The large T tails for the turbulent signals are exponential (see also Refs. 10, 25), that can be readily related to the Poisson character of the very large time periods. (This is difficult to reach technically in the white noise simulations.)

The similarity of shapes of $p(T)$, at least for the central part of the PDF, for the white noise and for turbulent signals suggests some similarities. Such a similarity is rather nontrivial because one might imagine a better correspondence,

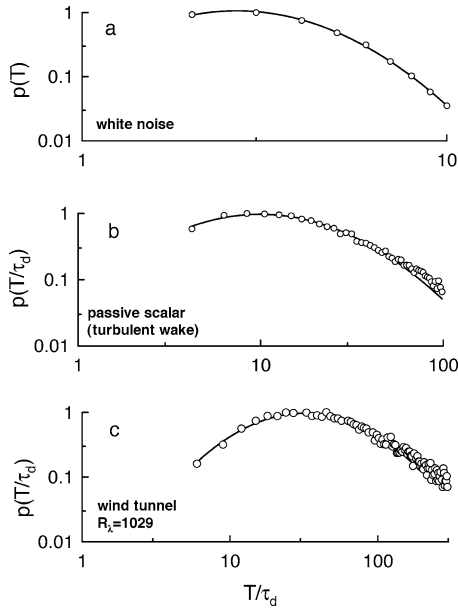


Fig. 7. Comparison of the white noise PDF (Fig. 7a) with those of the passive scalar signal in turbulent wake (Fig. 7b) and of the turbulent velocity signal (Fig. 7c). The *solid parabolas* (the best fit) indicate lognormal distribution, and τ_d is a dissipative scale for the signal.

instead, with the PDF of T for a stochastic signal with the Markov (Lorentzian) spectrum

$$E(f) = \frac{2\sigma}{1 + (f/f_0)^2}. \quad (11)$$

This expectation appears more natural because of the power-law spectrum characteristic of (11). But the Markov-Lorentzian signals exhibit power-law PDFs instead of exhibiting the logarithmical PDF.

We have come to the following conclusion after some careful scrutiny of many turbulent signals: the so-called *active* scalars (or vectors) in turbulent flows possess the properties of the Markov-Lorentzian scaling properties (cf. Ref. 3, where the cluster properties were explored). This conclusion is true for temperature in thermal convection, where the dynamics are determined by the heating, and also for the magnitude of magnetic field in magnetohydrodynamic turbulence. The scaling properties of the tendency to cluster for the ‘Markov-Lorentzian’ class is quite similar for the processes belonging to that class (see for an example of such behavior⁽³⁾) but significantly different from that of the ‘white noise’ class studied in present paper.

6. CONCLUDING REMARKS

Small-scale intermittency in turbulence has two ingredients: one due to amplitude variations and the other due to the tendency of structures to cluster together in space. For understanding the latter, it is useful to study the random telegraph approximation (TA) of the signal; by doing so, we eliminate amplitude variations and preserve only the information on clustering. Under benign conditions that should apply to turbulence far away from the walls, we have shown that there exists a unique relation between the spectral scaling of the signal and its TA. We have defined, and experimentally determined, the cluster exponents for the velocity and passive scalar signals and deduced their asymptotic values in the limit of infinite Reynolds number. The finite values of the asymptotic cluster exponents, for both the velocity and passive scalar, are a measure of the tendency of small-scales to cluster finitely even in the limit. Perhaps most importantly, the intermittency exponent of the dissipation is related to the cluster exponent through a ‘universal’ constant (see Eq. (8)). This is perhaps our most important qualitative conclusion. While its full implications are being explored, it appears that the amplitude effects are contained entirely in the one constant c whose numerical value we have determined empirically.

We have shown that there are two classes of signals, the white-noise type and the Markovian-Lorentzian type, which have two generically different behaviors for the probability density functions of the interpulse distance of the TA signals. The former is close to that for the velocity and passive scalars, while the latter is close to that for active scalars and vectors.

APPENDIX

Following the reasoning due to G.L. Eyink,⁽⁶⁾ we will show here that Eq. (1) can be supported by heuristic considerations. First, let us suppose for simplicity that the velocity is a monofractal with Hölder exponent h . It is well known⁽⁷⁾ that, for a wide class of signals, the fractal dimension of the zero-crossing set Z on the line is

$$D(Z) = 1 - h. \tag{A1}$$

The telegraph approximation

$$u(t) = \text{sign}(v(t)) \tag{A2}$$

of the velocity field $v(t)$ is bifractal, with “shocks” on the set Z with codimension h . Thus

$$\langle (\Delta u)^2 \rangle \sim l^h \tag{A3}$$

by the standard “bifractal” scaling argument (where Δu is variation of u on scale l). On the other hand,

$$\langle (\Delta v)^2 \rangle \sim l^{2h}. \quad (\text{A4})$$

In terms of the spectral exponents $n = 1 + 2h$ and $m = 1 + h$, this recovers the empirical relation (1). Equation (A1) provides also a restriction $n > 1$ that is significant for the application to the small-scale field such as vorticity.

For a multifractal signal

$$D(Z) = 1 - \zeta_1, \quad (\text{A5})$$

where ζ_1 is the first-order scaling exponent of $|\Delta u|$ (Theorem 4.2 of Ref. 5). Repeating the “bifractal” scaling argument, one expects that

$$\langle (\Delta u)^p \rangle \sim l^{\zeta_1} \quad (\text{A6})$$

for all $p > 1$, whereas

$$\langle (\Delta v)^p \rangle \sim l^{\zeta_p}. \quad (\text{A7})$$

Thus for multifractal signal one obtains

$$m = 1 + \zeta_1, \quad (\text{A8})$$

instead of the Eq. (1). For the case on hand, this will differ only slightly from the Eq. (1), see Ref. 24.

ACKNOWLEDGMENTS

The authors are grateful to G.G. Katul and to B.R. Pearson for the data and to A. Praskovsky for stimulating discussions. It is a special pleasure to dedicate the article to Jim Langer and Pierre Hohenberg on reaching the seventieth milestone.

REFERENCES

1. G. I. Barenblatt and N. Goldenfeld, *Phys. Fluids* **7**:3078 (1995).
2. J. T. Barnett and B. Kedem, *IEEE Trans. Inform. Theory* **37**:1188 (1991).
3. A. Bershadskii, J. J. Niemela, A. Praskovsky and K. R. Sreenivasan, *Phys. Rev. E* **69**:056314 (2004).
4. B. Castaing, Y. Gagne and E. J. Hopfinger, *Physica D* **46**:177 (1990).
5. A. Deliu and B. Jawerth, *Constr. Approx.* **8**:211 (1992).
6. G. Eyink, private communication.
7. K. J. Falconer, *The Geometry of Fractal Sets* (Cambridge University Press, Cambridge, 1985).
8. G. Falkovich and K. R. Sreenivasan, *Phys. Today* **59**:43 (2006).
9. M. Hinich, *Technometrics* **9**:391 (1967).
10. P. Kailasnath and K. R. Sreenivasan, *Phys. Fluids* **5**:2879 (1993).
11. P. Kailasnath, K. R. Sreenivasan and J. R. Saylor, *Phys. Fluids A* **5**:3207 (1993).
12. G. G. Katul, C. I. Hsieh and J. Sigmon, *Boundary Layer Meteor.* **82**:49 (1997).

13. A. N. Kolmogorov, *Dokl. Akad. Nauk. SSSR* **30**:9–13 (1941); reproduced in Proc. Roy. Soc. A **434**:9–14 (1991).
14. M. R. Leadbetter and J. D. Gryer, *Bull. Am. Math. Soc.* **71**:561 (1965).
15. V. S. Lvov and I. Procaccia, *Phys. Rev. Lett.* **74**:2690 (1995).
16. G. Molchan, private communication.
17. A. S. Monin and A. M. Yaglom, *Statistical Fluid Mechanics*, Vol. 2 (MIT Press, Cambridge, 1975).
18. A. M. Obukhov, *J. Fluid Mech.* **13**:77 (1962).
19. B. R. Pearson, P.-A. Krogstad and W. van de Water, *Phys. Fluids* **14**:1288 (2002).
20. A. Praskovskiy and S. Oncley, *Fluid Dyn. Res.* **21**:331 (1997).
21. K. R. Sreenivasan, *Phys. Fluids* **27**:1048 (1984).
22. K. R. Sreenivasan, R. A. Antonia and D. Britz, *J. Fluid Mech.* **94**:745 (1979).
23. K. R. Sreenivasan and A. Bershadskii, *J. Fluid Mech.* **554**:477 (2006).
24. K. R. Sreenivasan and B. Dhruva, *Prog. Theor. Phys. Suppl.* **130**:103 (1998).
25. K. R. Sreenivasan, A. Prabhu and R. Narasimha, *J. Fluid. Mech.* **137**:251 (1983).